Published online 2 March 2017

Nucleic Acids Research, 2017, Vol. 45, No. 11 ***e98***
doi: 10.1093/nar/gkx154

Targeted gene knock-in by homology-directed genome editing using Cas9 ribonucleoprotein and AAV donor delivery

Thomas Gaj[1,†], Brett T. Staahl[2,†], Gonçalo M. C. Rodrigues[1,3], Prajit Limsirichai[4], Freja K. Ekman[5], Jennifer A. Doudna[2,5,6,7,*] and David V. Schaffer[1,8,9,*]

[1]Department of Bioengineering, University of California, Berkeley, Berkeley, CA 94720, USA, [2]Department of Molecular and Cell Biology, University of California, Berkeley, CA 94720, USA, [3]Department of Bioengineering and Institute for Bioengineering and Biosciences, Instituto Superior Técnico, Universidade de Lisboa, 1049-001 Lisbon, Portugal, [4]Department of Plant and Microbial Biology, University of California, Berkeley, Berkeley, CA 94720, USA, [5]Department of Chemistry, University of California, Berkeley, Berkeley, CA 94720, USA, [6]Howard Hughes Medical Institute, University of California, Berkeley, Berkeley, CA 94720, USA, [7]MBIB Division, Lawrence Berkeley National Laboratory, Berkeley, CA 94720, USA, [8]Department of Chemical and Biomolecular Engineering, University of California, Berkeley, Berkeley, CA 94720, USA and [9]Helen Wills Neuroscience Institute, University of California, Berkeley, Berkeley, CA 94720, USA

Received December 16, 2016; Revised February 18, 2017; Editorial Decision February 21, 2017; Accepted February 22, 2017

ABSTRACT

Realizing the full potential of genome editing requires the development of efficient and broadly applicable methods for delivering programmable nucleases and donor templates for homology-directed repair (HDR). The RNA-guided Cas9 endonuclease can be introduced into cells as a purified protein in complex with a single guide RNA (sgRNA). Such ribonucleoproteins (RNPs) can facilitate the high-fidelity introduction of single-base substitutions via HDR following co-delivery with a single-stranded DNA oligonucleotide. However, combining RNPs with transgene-containing donor templates for targeted gene addition has proven challenging, which in turn has limited the capabilities of the RNP-mediated genome editing toolbox. Here, we demonstrate that combining RNP delivery with naturally recombinogenic adeno-associated virus (AAV) donor vectors enables site-specific gene insertion by homology-directed genome editing. Compared to conventional plasmid-based expression vectors and donor templates, we show that combining RNP and AAV donor delivery increases the efficiency of gene addition by up to 12-fold, enabling the creation of lineage reporters that can be used to track the conversion of striatal neurons from human fibroblasts in real time. These results thus illustrate the potential for unifying nuclease protein delivery with AAV donor vectors for homology-directed genome editing.

INTRODUCTION

In recent years, the RNA-guided Cas9 endonuclease (1) from type II clustered regularly interspaced short palindromic repeats (CRISPR)-CRISPR-associated (Cas) systems has emerged as a versatile and efficient genome editing platform (2). Cas9 can be directed to nearly any genomic location to induce a DNA double-strand break (DSB) via RNA–DNA complementary base pairing using a single guide RNA (sgRNA) (3–5). DSBs induced by Cas9 or other programmable nuclease platforms (6,7) are processed by the cellular DNA repair machinery, typically through non-homologous end joining (NHEJ) (8) or homology-directed repair (HDR) (9). Whereas NHEJ is employed primarily to disrupt gene expression through the introduction of random base insertions and/or deletions (indels) (10,11), HDR can be harnessed to mediate gene correction (12,13) or targeted gene addition (14). This is achieved using a homologous single or double-stranded DNA donor template, which is delivered alongside Cas9 and serves as a substrate for DNA repair. However, despite its broad potential to enable and accelerate many basic and clinical research applications, HDR-mediated genome editing remains inefficient and limited by several factors, including the efficiency of Cas9 and donor DNA delivery (15), the suitability of plas-

*To whom correspondence should be addressed. Tel: +1 510 642 4923; Fax: +1 510 642 4923; Email: schaffer@berkeley.edu
Correspondence may also be addressed to Jennifer A. Doudna. Tel: +1 510 643 0225; Fax: +1 510 643 0080; Email: doudna@berkeley.edu
†These authors contributed equally to the paper as first authors.

© The Author(s) 2017. Published by Oxford University Press on behalf of Nucleic Acids Research.
This is an Open Access article distributed under the terms of the Creative Commons Attribution License (http://creativecommons.org/licenses/by-nc/4.0/), which permits non-commercial re-use, distribution, and reproduction in any medium, provided the original work is properly cited. For commercial re-use, please contact journals.permissions@oup.com

Downloaded from https://academic.oup.com/nar/article-abstract/45/11/e98/3059660/Targeted-gene-knock-in-by-homology-directed-genome
by Undergraduate Library user
on 13 October 2017

mid DNA as a donor template for HDR (16) and the phase of the cell cycle in which DNA cleavage occurs in (17).

Both Cas9 and its sgRNA can be introduced into cells as a pre-formed ribonucleoprotein (RNP) complex via nucleofection (18–20) or lipid-mediated transient transfection (21,22). Similar to cell-penetrating zinc-finger (23–25) and transcription-activator like effector (TALE) nuclease proteins (26), RNPs cleave DNA almost immediately upon cell entry, and are degraded shortly thereafter (18). In fact, due to their rapid action and fast turnover, RNPs yield fewer off-target effects than methods that rely on transient expression from nucleic acids (18,19,21). Moreover, RNPs can be complemented with recombinogenic single-stranded DNA oligonucleotides (27), enabling the introduction of single-base substitutions via HDR (18–21,28). Yet despite their flexibility, efforts to combine RNPs with transgene-containing donor templates for targeted gene addition have thus far proven unsuccessful. Given the breadth of applications possible for nuclease-driven transgenesis, as well as the advantages afforded by RNP delivery, this incompatibility has emerged as a considerable gap within the RNP genome editing toolbox.

In addition to their capacity to safely mediate gene delivery (29), adeno-associated virus (AAV) vectors are endowed with the unique ability to stimulate gene targeting via homologous recombination (HR) (16,30,31), even in the absence of a nuclease-induced DSB. AAVs are non-pathogenic and non-enveloped single-stranded DNA viruses capable of transducing both dividing and non-dividing cells. The AAV viral genome is approximately 4.7 kilobases (kb) in length and contains two inverted terminal repeats (ITRs) that flank two open reading frames, *rep* and *cap*. To generate recombinant AAV vectors capable of mediating gene targeting, the AAV viral genome is replaced with a donor cassette carrying the desired genomic modification flanked by sequences homologous to a specific genomic site (31). Both the *rep* and *cap* genes are then provided *in trans* along with adenoviral helper genes to facilitate the production of recombinant AAV particles harboring the designed donor template. Given their innate ability to induce activation of the cellular DNA repair pathway and promote gene targeting (32), we reasoned that AAV donor vectors would serve as a suitable repair template for DSBs induced by RNP.

In the present study, we demonstrate that combining RNP and AAV donor delivery enables efficient genome editing—including targeted gene addition—via HDR. This approach facilitated both gene correction and the knock-in of reporter genes into the rat nestin and human DARPP-32 genes, the latter of which enabled the conversion of striatal neurons from human fibroblasts to be tracked in real time. Our results thus illustrate the potential for uniting RNP and AAV donor delivery for efficient homology-directed genome editing.

MATERIALS AND METHODS

Plasmid construction

Construction of the lentiviral vector encoding GFPΔ35 (pLV-GFPΔ35) and the AAV vector carrying the t37GFP repair template (pAAV-t37GFP) was previously described (33). Homology arms for the nestin and DARPP-32 genes were generated by nested polymerase chain reaction (PCR) using genomic DNA harvested from rat C6 cells or human adult dermal fibroblasts, respectively, using the primers described in Supplementary Table S1. To construct the DARPP-32 donor template, the enhanced green fluorescent protein (EGFP) and puromycin-resistance genes were PCR amplified from pAAV-NKX2.2-EGFP using the primers DARPP-32-Cargo-Fwd and DARPP-32-Cargo-Rev, and fused to both the 'left' and 'right' homology arms to the DARPP-32 locus by overlap PCR. To construct the nestin donor template, the cytomegalovirus (CMV) promoter was PCR amplified from pAAV-CAGGS-EGFP (Addgene #22212) (34) and ligated into the KpnI and AgeI restriction sites of the plasmid pAAV-NKX2.2-EGFP. The EGFP and the puromycin-resistance genes were then PCR amplified using the primers Nestin-Cargo-Fwd and Nestin-Cargo-Rev, and fused to both the 'left' and 'right' homology arms to the nestin locus by overlap PCR. Primer sequences are provided in Supplementary Table S1. The resulting PCR products, which encoded a promoterless EGFP gene and a puromycin-resistance gene under the control of a CMV or phosphoglycerate kinase (PGK) promoter flanked by nestin or DARPP-32 homology arms, respectively, were digested and ligated into the BamHI and XhoI restriction sites of pAAV-CAG-EGFP. The sequences of the rat nestin and human DARPP-32 targeting constructs are provided in Supplementary Tables S2 and 3, respectively.

Oligonucleotides encoding sgRNAs targeting GFPΔ35, as well as the nestin and DARPP-32 genes were custom synthesized (Elim Biopharm) and phosphorylated by T4 polynucleotide kinase (New England Biolabs; NEB) for 30 min at 37°C. Oligonucleotides were annealed for 5 min at 95°C, cooled to room temperature and ligated into the BsmBI restriction sites of pX330-U6-Chimeric-BB-CBh-hSpCas9 (Addgene #42230) (3). Correct construction of all plasmids was verified by Sanger sequencing (UC Berkeley DNA Sequencing Facility).

Cell culture

Human embryonic kidney (HEK) 293T and U2OS cells (UC Berkeley Tissue Culture Facility), C6 cells (kindly provided by S. Kumar) and human adult dermal fibroblasts (hFbs; ScienCell) were maintained in Dulbecco's modified Eagle's medium (DMEM; Corning and Thermo-Fisher) supplemented with 10% (vol/vol) fetal bovine serum (FBS; Thermo-Fisher) and 1% (vol/vol) Antibiotic-Antimycotic (Anti-Anti; Thermo-Fisher) in a humidified 5% CO_2 atmosphere at 37°C. To generate the HEK293T-GFPΔ35 and U2OS-GFPΔ35 reporter cell lines, HEK293T and U2OS cells were transduced with a lentiviral vector encoding GFPΔ35 (LV-GFPΔ35) followed by limiting dilution in serum-containing media with 1 μg/ml of puromycin (Sigma-Aldrich). Based on the number of cells that survived antibiotic selection, we estimated that each cell line contained a single copy of the reporter gene. To generate LV-GFPΔ35, HEK293T cells were seeded onto a 15-cm dish and transfected with 10 μg of pLV-GFPΔ35, 5 μg of pMDL g/p RRE, 3.5 μg of pMD2.G and 1.5 μg of pRSV-Rev using 120 μl of polyethylamine (1 μg/μl; PEI). At 48 h after transfection, cell culture medium was harvested, virions

Downloaded from https://academic.oup.com/nar/article-abstract/45/11/e98/3059660/Targeted-gene-knock-in-by-homology-directed-genome
by Undergraduate Library user
on 13 October 2017

were concentrated by ultracentrifugation (L8-55M Ultracentrifuge; Beckman Coulter), resuspended in phosphate-buffered saline (PBS) with 20% sucrose (Sigma-Aldrich) and applied onto HEK293T and U2OS cells.

Cas9 protein expression and purification

The Cas9 protein from *Streptococcus pyogenes* (SpCas9) was expressed from pMJ915 (Addgene #69090) in *Escherichia coli* Rosetta 2 cells (EMD Millipore) and purified as previously described (1). Cas9 protein was stored at -80°C in cryopreservation buffer (20 mM HEPES, 150 mM KCl, 1 mM TCEP, 10% glycerol, pH 7.5).

sgRNA *in vitro* transcription

The DNA templates for *in vitro* transcription encoding the sgRNA were assembled using synthetic oligonucleotides as previously described (19). Additionally, *in vitro* transcription and RNA purification were performed as previously described (19).

Cas9 RNP assembly

To prepare RNP, Cas9 protein was incubated with sgRNA (1:1.2 molar ratio) in RNP buffer (20 μM HEPES, 150 mM KCl, 1 mM TCEP, 1 mM $MgCl_2$, 10% glycerol, pH 7.5) for 10 min at 37°C. Following incubation, RNP was centrifuged at 15 000 × *g* for 1 min using a 0.22 μm Costar Spin-X Centrifuge Tube Filter (Costar) according to the manufacturer's instructions. RNP was concentrated to ∼20–40 μl using an Ultra-0.5 ml Centrifugal Filter Unit (Amicon) at 14 000 × *g* for 3 min.

AAV vector production

AAV vectors were produced as previously described (35). Briefly, HEK293T cells were seeded onto 15-cm plates at a density of 3×10^7 cells per plate in serum-containing medium. At 16–24 h after seeding, cells were transfected with 15 μg of pAAV-t37GFP, 15 μg of rAAV1 and 15 μg of pHelper using 135 μl of PEI (1 μg/μl). After 72 h, cells were harvested using a cell scraper and centrifuged at 4000 × *g* for 5 min at room temperature. Medium was then removed, and cell pellets were resuspended in 2 ml of AAV lysis buffer (50 mM Tris–HCl, 150 mM NaCl, pH 8.0) per plate. Cells were lysed by freeze-thaw using a dry-ice ethanol and 37°C water bath. Lysate was then incubated with 10 Units (U) of Benzonase (Sigma-Aldrich) per milliliter of lysate for 30 min at 37°C, and centrifuged at 10 000 × *g* for 10 min at room temperature. Lysate supernatant was collected and overlaid onto an iodixanol density gradient (OptiPrep Density Gradient Medium; Sigma-Aldrich), and vector was purified by ultracentrifugation, as described (35). Extracted AAV vector was washed three times with 15 ml of PBS with 0.001% Tween-20 (Sigma-Aldrich) using an Ultra-15 Centrifugal Filter Unit (Amicon) at 4000 × *g* and concentrated to ∼200 μl. AAV was stored at 4°C. Viral genomic titer was determined by quantitative real-time PCR using SYBR Green with the primers qPCR-EGFP-Fwd and qPCR-EGFP-Rev (Supplementary Table S1).

AAV-RNP delivery

HEK293T-GFPΔ35, U2OS-GFPΔ35 and C6 were seeded onto 96-well plates at a density of 2×10^5 cells per well in serum-containing medium with 200 ng/ml of nocodazole (Sigma-Aldrich). After 30 min, the AAV donor vector (t37EGFP-AAV1 for HEK293T-GFPΔ35 and U2OS-GFPΔ35, and nestin-AAV1 for C6) was added onto cells in the presence of 200 ng/ml of nocodazole. After 16 h, cells were dissociated with 0.05% trypsin (Thermo-Fisher), centrifuged at 400 × *g* for 3 min, washed once with PBS and resuspended in 20 μl of Nucleofector Solution SF (Lonza) with 10 μl of RNP. Cells were nucleofected using the Amaxa 96-well Shuttle system (Lonza) and the program CM120. Immediately after nucleofection, 100 μl of serum-containing medium was added to nucleofected wells, and cells were transferred into a fresh 96-well plate until further use. HEK293T-GFPΔ35 and U2OS-GFPΔ35 were maintained in serum-containing medium, and C6 cells were maintained in serum-containing medium with 50 ng/ml of FGF-2.

Flow cytometry

HEK293T-GFPΔ35, U2OS-GFPΔ35 and C6 cells were washed once with PBS, harvested with 0.05% trypsin and transferred into a fresh 96-well plate containing 100 μl of serum-containing medium. Samples were evaluated using a LSRFortessa X-20 cell analyzer with a High-Throughput Sampler adapter (BD Biosciences; UC Berkeley Flow Cytometry Core Facility). Data were collected for 20 000 live events per sample and analyzed using FlowJo software (FlowJo LLC).

Surveyor nuclease assay

HEK293T-GFPΔ35 and C6 cells were harvested 72 h after AAV-RNP delivery or plasmid transfection, and genomic DNA was isolated using QuickExtract DNA Extraction Solution (Epicentre), according to the manufacturer's instructions. The GFPΔ35 and nestin genomic loci were amplified by nested PCR using the Expand High Fidelity Taq System (Roche). Primer sequences are provided in Supplementary Table S1. Following PCR, the Surveyor Mutation Detection Kit (Integrated DNA Technologies) was used according to the manufacturer's instructions. Cleavage products were visualized by non-denaturing TBE-PAGE, and the gene modification frequency was measured as the ratio of cleaved to uncleaved product, as described (36). Band intensity was quantified using ImageJ software (https://imagej.nih.gov/ij/).

Neural differentiation

The plasmids phMYT1L-N106 (Addgene #60861), phDLX1-N174 (Addgene #60859), phDLX2-N174 (Addgene #60860) and pmCTIP2-N174 (Addgene #60858) express MYT1L, DLX1, DLX2 and CTIP2, respectively, under the control of a human elongation factor-1 alpha (EF1a) promoter. The plasmid pTight-9-124-BclxL (Addgene #60857) expresses a synthetic cluster of miR-9/9* and miR-124 fused to Bcl-XL under the control

Downloaded from https://academic.oup.com/nar/article-abstract/45/11/e98/3059660/Targeted-gene-knock-in-by-homology-directed-genome
by Undergraduate Library user
on 13 October 2017

of a doxycycline-inducible promoter, and the plasmid rtTA-N144 (Addgene #66810) expresses the reverse tetracycline-controlled transactivator (rtTA) alongside a hygromycin-resistance gene. Lentiviral vectors were packaged and purified as described above. Concentrated virus was stored as single-use aliquots at −80°C.

hFbs (ScienCell) were maintained in DMEM (Thermo-Fisher) supplemented with 10% FBS (Hyclone), 0.01% β-mercaptoethanol, 1% non-essential amino acids, 1% sodium pyruvate, 1% GlutaMAX, 10 mM HEPES and 1% Penicillin-Streptomycin (all from Thermo-Fisher) in a humidified 5% CO_2 atmosphere at 37°C. For synchronization, fibroblasts were treated with 2 μg/ml of aphidicolin for 18 h, washed once with PBS, incubated in serum-containing medium at 37°C for 8 h and then treated with a second dose of aphidicolin. At the same time, AAV donor vector (DARPP-32-AAV1) was added onto cells in the presence of 1 μM Scr7 (Xcessbio Biosciences). After 16 h, cells were dissociated with 0.05% trypsin, centrifuged at 400 × *g* for 3 min, washed once with PBS and resuspended in 20 μl of Nucleofector Solution P2 (Lonza) with 10 μl of RNP. Cells were nucleofected using the Amaxa 96-well Shuttle system and the program FP125. Immediately after nucleofection, 100 μl of serum-containing medium was added to nucleofected wells and cells were transferred onto gelatin-coated wells and maintained at 37°C. After 5 days, 1 μg/ml of puromycin was added to the cell culture medium for 10 days before cells were transferred onto gelatin-coated 12-well plates (Greiner) at a density of 2 × 10^5 cells per well in serum-containing medium. The following day, cells were transduced with lentiviral vectors encoding miR-9/9*-124 and Bcl-XL, CTIP2, DLX1, DLX2, MYT1L and rtTA in the presence of 8 μg/ml of polybrene. After 16 h, cells were incubated with fresh serum-containing medium with 1 μg/ml of doxycycline (Sigma-Aldrich) to induce miR-9/9*-124 expression and maintained at 37°C. After 48 h, cells were dissociated with 0.25% trypsin (Thermo-Fisher) and re-seeded onto poly-ornithine (0.01%; Sigma-Aldrich), laminin (5 μg/ml; Roche) and fibronectin (2 μg/ml; Sigma-Aldrich)-coated glass coverslips in serum-containing medium with 1 μg/ml of doxycycline. The following day, medium was changed to Neuronal Media (ScienCell) supplemented with 1 mM of valproic acid (Calbiochem), 400 μM of dibutyryl-cAMP (Sigma-Aldrich), 10 ng/ml of human brain-derived neurotrophic factor (Peprotech), 10 ng/ml of human neurotrophin-3 (Peprotech) and 1 μM of retinoic acid (Sigma-Aldrich, 1 μM) with the appropriate antibiotics (37). Neuronal Media was replenished every 4 days by replacing half of the media with an equal volume of fresh media, and doxycycline was replenished every two days for ∼4 weeks. Addition of antibiotics was terminated after 2 weeks.

Digital droplet PCR

hFbs were harvested and genomic DNA was purified using the DNeasy Blood & Tissue Kit (Qiagen) and quantitated using a Nanodrop Spectrophotometer. The digital droplet PCR (ddPCR) reaction mixture was prepared with the following: 1× ddPCR supermix for probes (no dUTP; Bio-Rad), 900 nM of DARPP-32 forward primer (FAM), 900 nM of DARPP-32 reverse primer (FAM), 900 nM of human RPP30 CNV assay reference primers (HEX; all probes purchased from Bio-Rad; Supplementary Table S1) and 50 ng of genomic DNA. DG8 Cartridges (Bio-Rad) were filled with ddPCR reaction mixtures and Droplet Generation Oil for Probes (Bio-Rad). Droplets were generated using a QX200 Droplet Generator (Bio-Rad), according to the manufacturer's instructions and then transferred into a 96-well PCR plate for PCR using a T100 Thermal Cycler (Bio-Rad). The following thermal cycle program was used: step 1, 95°C for 10 min; step 2, 94°C for 30 s; step 3, 52°C for 1 min; step 4, 72°C for 2 min; repeat steps 2–4 39 times, step 5, 98°C for 10 min. Following PCR, droplets were analyzed using a QX200 Droplet Reader (Bio-Rad) and data was evaluated using QuantaSoft software (Bio-Rad).

Immunocytochemistry

Five weeks after lentiviral transduction, cells grown on poly-ornithine-, laminin- and fibronectin-coated glass coverslips were fixed with 4% (w/v) paraformaldehyde and then incubated overnight with primary antibodies in blocking solution (2% normal goat serum [Sigma-Aldrich], 2% bovine serum albumin and 0.1% Triton X-100). Stained cells were washed three times with PBS and incubated with secondary antibodies for 2 h at room temperature followed by a 10 min incubation with DAPI. Cells were mounted using 4% n-propyl gallate (Sigma) in 90% glycerol and 10% PBS and imaged using an EVOS FL Imaging System (Thermo-Fisher). The following primary antibodies were used: rabbit anti-DARPP-32 (1:400, Cell Signaling, 19A3) and mouse anti-MAP2-HM2 (1:5000, Sigma-Aldrich, M9942). The following secondary antibodies were used: goat anti-rabbit Alexa Fluor 568 (Thermo-Fisher, A-11011) and goat anti-mouse Alexa Fluor 647 (Thermo-Fisher, A-21235).

Statistics

Data are means and error bars were calculated as standard deviation. Unpaired *t*-tests were performed using Prism 7 (GraphPad Software).

RESULTS

Combining Cas9 ribonucleoprotein and AAV donor delivery enables homology-directed genome editing via HDR

To determine whether RNP and AAV donor co-delivery could facilitate homology-directed genome editing, we established a GFP reporter system (38) to assess and quantify gene correction via HDR. To achieve this, we modified HEK293T cells to stably express a GFP gene that was disabled by the presence of a 35-bp insertion containing a stop codon and frameshift mutation (hereafter referred to as GFPΔ35) (Figure 1A). We then generated an sgRNA targeting the 35-bp insertion in GFPΔ35, as well as an AAV donor template (t37GFP) capable of mediating its correction. The donor consisted of a promoter-less GFP transgene with a 37-bp deletion at the 5′ portion of its coding sequence that rendered it non-functional, and 290 and 1619 nt of homology upstream and downstream the sgRNA

Downloaded from https://academic.oup.com/nar/article-abstract/45/11/e98/3059660/Targeted-gene-knock-in-by-homology-directed-genome
by Undergraduate Library user
on 13 October 2017

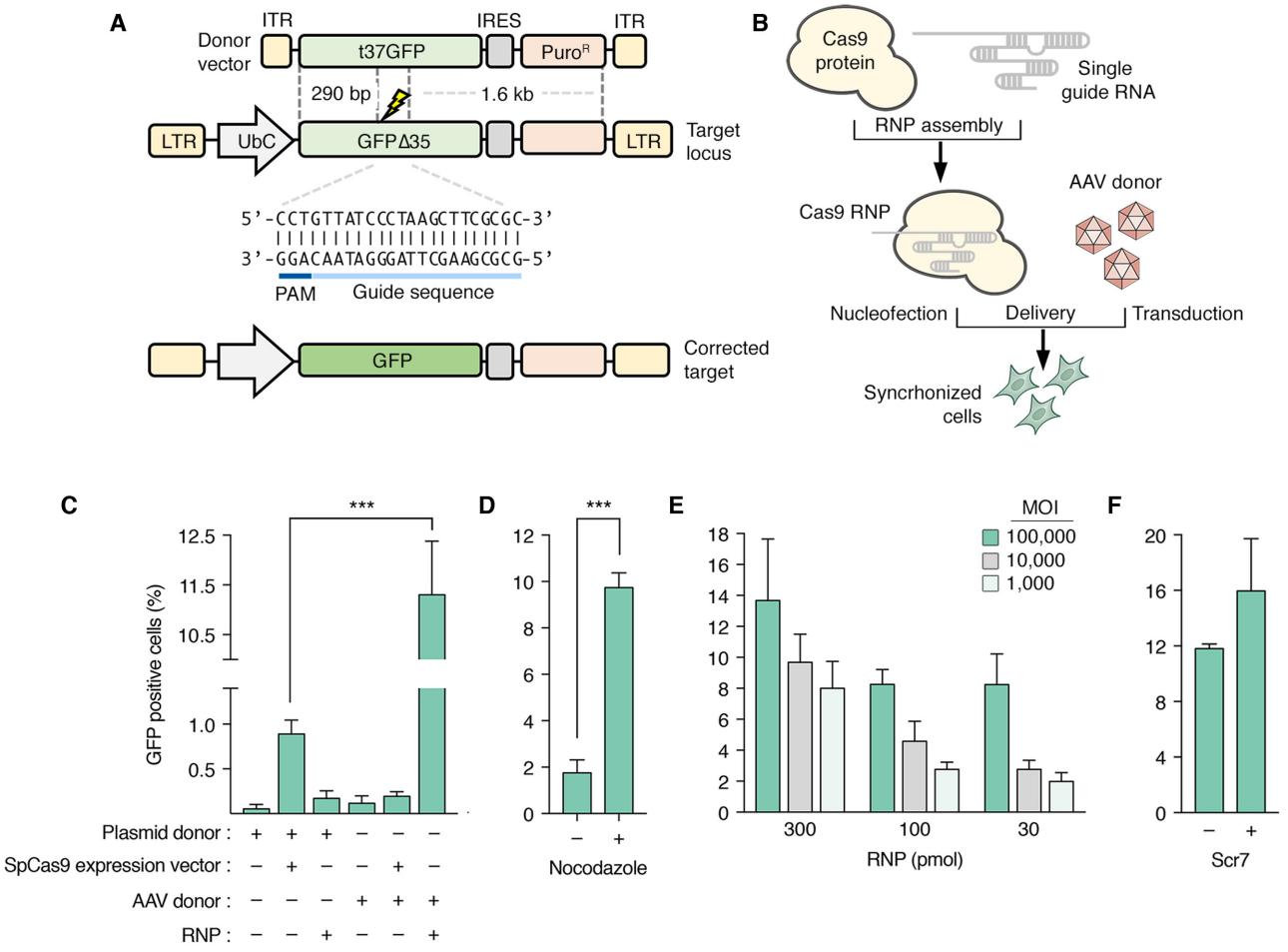

Figure 1. Combining Cas9 ribonucleoprotein (RNP) and adeno-associated virus (AAV) donor delivery facilitates gene correction in HEK293T cells. (**A**) Schematic representation of the GFP reporter system. Lightning bolt indicates approximate position of the RNP cleavage site. The sgRNA target site in GFPΔ35 is shown. Abbreviations are as follows: ITR, inverted terminal repeat; IRES, internal ribosome entry site; LTR, long terminal repeat; UbC, ubiquitin C promoter; PAM, protospacer adjacent motif. (**B**) Cartoon illustrating RNP and AAV delivery to cells synchronized at G2/M phase. (**C**) Percentage of GFP positive HEK293T reporter cells following delivery of different combinations of plasmid donor (800 ng), Cas9–sgRNA expression vector (800 ng), AAV donor (multiplicity of infection [MOI] = 100 000) and RNP (300 pmol). (**D**) Percentage of GFP positive reporter cells following treatment with RNP (300 pmol) and AAV donor (MOI = 100 000) in the presence or absence of 200 ng/ml nocodazole. (**E** and **F**) Percentage of GFP positive reporter cells following treatment with (E) increasing amounts of RNP and AAV donor or (F) RNP (300 pmol) and AAV donor (MOI = 100 000) in the presence or absence of 1 μM Scr7. In all cases, AAV donor was added to cells 16 h before RNP delivery. All cells were treated with 200 ng/ml of nocodazole unless otherwise indicated. Values are means ($n = 3$) and error bars indicate S.D. ***$P < 0.0005$; unpaired t-tests.

target site in GFPΔ35, respectively (Figure 1A). Importantly, transfection of HEK293T reporter cells with an RNP composed of the SpCas9 nuclease and an sgRNA targeting GFPΔ35 resulted in the introduction of indels in the GFPΔ35 locus (Supplementary Figure S1), indicating the functionality of the Cas9–sgRNA complex.

We transduced HEK293T reporter cells with the t37GFP donor vector and then nucleofected cells with RNP containing the GFPΔ35-targeting sgRNA. This donor template was packaged into AAV serotype 1 (AAV1), which transduces a range of transformed and primary cell types in culture (39). Importantly, since transduction efficiency can vary depending on the target cell type and the AAV serotype being employed, it may be necessary to screen for the optimal AAV variant for a specific application. Timed delivery of RNP via cell cycle synchronization was previously shown to enhance HDR with a single-stranded DNA oligonucleotide (19). We thus also treated reporter cells with nocodazole, a microtubule inhibitor that arrests mitotic cells at G2/M phase (40), prior to AAV-RNP delivery (Figure 1B).

Notably, we found that ∼11% of reporter cells were GFP$^+$ following transduction with a high dose of AAV donor (multiplicity of infection [MOI] = 100 000) and RNP (300 pmol) (Figure 1C). Because we routinely observe ∼90% transfection efficiency in HEK293T cells using PEI or nucleofection, this MOI is analogous to transfecting 1×10^6 cells with 800 ng of the equivalent donor plasmid (which is ∼6.8 kb in size). Importantly, despite its well-documented ability to stimulate HDR in the absence of a nuclease-induced DSB (16,30), we observed near background levels of GFP expression in cells treated with AAV vector only. Negligible amounts of gene correction were also observed when RNP was combined with a plasmid-based donor template, or when a Cas9–sgRNA expression vector was com-

Downloaded from https://academic.oup.com/nar/article-abstract/45/11/e98/3059660/Targeted-gene-knock-in-by-homology-directed-genome
by Undergraduate Library user
on 13 October 2017

bined with an AAV donor template (Figure 1C). Specifically, AAV-RNP delivery yielded ∼10-fold more GFP$^+$ cells in comparison to cells nucleofected with a plasmid donor alongside an expression vector encoding Cas9 and the GFPΔ35-targeting sgRNA ($P < 0.0005$) (Figure 1C), indicating the ability of AAV-RNP to enhance homology-directed genome editing.

Optimization of AAV-RNP delivery

To determine the optimal time point for administering AAV donor relative to RNP, we treated HEK293T reporter cells with t37GFP-AAV1 (MOI = 100 000) at 16, 4 and 0 h before RNP delivery. No significant difference ($P > 0.5$) in the number of GFP$^+$ cells was observed between any of the conditions tested (Supplementary Figure S2), suggesting an intrinsic flexibility to AAV-RNP delivery that could accommodate various experimental timelines. We also evaluated the importance of cell synchronization on AAV-RNP delivery by withholding nocodazole from reporter cells treated with both factors. This resulted in a ∼5-fold decrease in the number of GFP$^+$ cells ($P < 0.0005$) (Figure 1D), illustrating the importance of employing cell synchronization to maximize HDR in mitotic cells. Additionally, we found that the frequency of genome editing via HDR was dependent on the dose of both AAV donor and RNP (Figure 1E). This analysis revealed that up to 2% of reporter cells underwent gene correction when treated with our lowest dose of AAV donor (MOI = 1000) and RNP (30 pmol) (Figure 1E), suggesting a degree of tunability to AAV-RNP delivery that could be leveraged to reduce off-target effects, particularly since the off-target activity of a nuclease is proportional to its concentration within a cell (23).

To further enhance genome editing via HDR, we explored the possibility of combining AAV-RNP delivery with Scr7, a small molecule inhibitor of DNA ligase IV (41), a key component of the NHEJ repair pathway. Inhibition of DNA ligase IV by Scr7 was previously reported to enhance the efficiency of HDR following Cas9-induced DNA cleavage in several mammalian cell lines (42,43). We found that up to 16% of reporter cells were GFP$^+$ following treatment with our highest dose of AAV (MOI = 100 000) and RNP (300 pmol) in the presence of Scr7, increasing the percentage of GFP$^+$ cells by ∼5% in comparison to cells not treated with Scr7 (Figure 1E). These results underscore the potential for unifying different methods that enhance HDR as means to improve the efficiency of genome editing.

We also evaluated the generality of AAV-RNP delivery by adapting the GFP reporter system described above to U2OS cells, a human bone osteosarcoma epithelial cell line routinely used to evaluate genome editing outcomes. We found that ∼18% of U2OS reporter cells were GFP$^+$ following t37GFP-AAV1 (MOI = 100 000) and RNP (300 pmol) delivery, and that the extent of gene correction was dependent on the dose of AAV vector administered to cells (Figure 2A). Moreover, similar to observations in HEK293T cells, we found that Scr7 further increased the frequency of gene editing via HDR in U2OS reporter cells, yielding up to 22% GFP$^+$ cells following treatment with AAV (MOI = 100 000) and RNP (300 pmol) (Figure 2B).

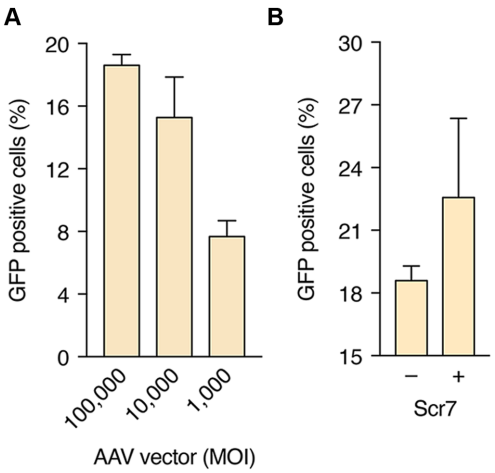

Figure 2. Gene correction in U2OS following RNP and AAV donor delivery. (**A** and **B**) Percentage of GFP positive reporter cells following treatment with (A) RNP (300 pmol) and increasing amounts of AAV donor or (B) RNP (300 pmol) and AAV donor (MOI = 100 000) in the presence or absence of 1 μM Scr7. AAV donor was added to cells 16 h before RNP delivery. All cells were treated with 200 ng/ml of nocodazole. Values are means ($n = 3$) and error bars indicate S.D.

Knock-in of EGFP into the nestin locus via AAV-RNP delivery

We next determined whether AAV-RNP delivery could be harnessed to facilitate knock-in of a transgene into an endogenous genomic locus. Based on our interest in neurogenesis and its role in learning and memory (44), we targeted the rat nestin gene, which encodes an intermediate filament protein routinely used as a neural stem/progenitor cell marker. We designed a sgRNA targeting the 3′ end of the last exon of the nestin gene, and constructed a donor template containing a promoter-less EGFP gene that would be expressed as an in-frame fusion with nestin (Figure 3A). This donor also contained a puromycin-resistance gene under the control of a CMV promoter, and ∼1000 and ∼1100 nt of homology to the nestin locus upstream and downstream the sgRNA target site, respectively (Figure 3A). Critically, since the EGFP gene in the donor lacks a promoter to drive its expression, only those cells correctly targeted by AAV would produce EGFP, since its expression would be controlled by the nestin promoter.

We transduced rat C6 glioma cells with a nestin-AAV1 donor (MOI = 100 000) and RNP (300 pmol) complexed with our most efficient nestin-targeting sgRNA (Supplementary Figure S3). To quantify the knock-in frequency, we cultured C6 cells with fibroblast growth factor-2 (FGF-2), which upregulates nestin expression (45), immediately after AAV-RNP delivery. The percentage of EGFP$^+$ cells, which was expected to correlate with the HDR frequency, was then measured by flow cytometry 72 h after AAV-RNP delivery. Notably, compared to nucleofection of a plasmid donor and a Cas9–sgRNA expression vector, we observed a ∼12-fold increase in the number of GFP$^+$ cells using AAV-RNP ($P < 0.0005$) (Figure 3B). Up to 4% of C6 cells treated by AAV-RNP in conjunction with Scr7 were EGFP$^+$ (Figure 3B). Critically, no difference in indel formation was observed be-

Downloaded from https://academic.oup.com/nar/article-abstract/45/11/e98/3059660/Targeted-gene-knock-in-by-homology-directed-genome
by Undergraduate Library user
on 13 October 2017

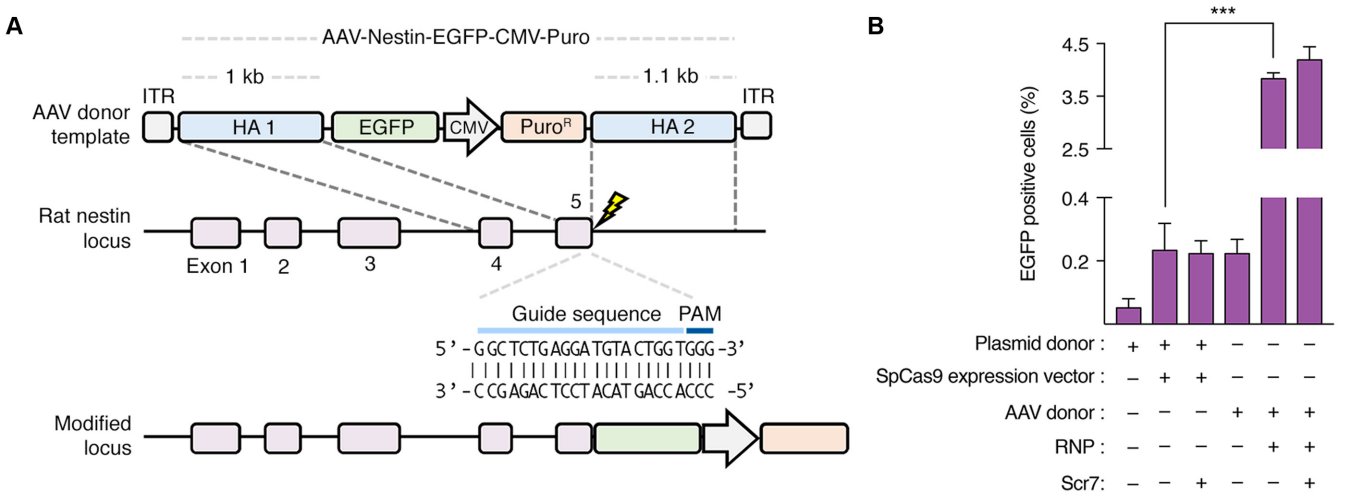

Figure 3. EGFP knock-in into the rat nestin locus via RNP and AAV donor delivery. (**A**) Schematic representation of the strategy used to tag the rat nestin gene with EGFP. Lightning bolt indicates approximate position of the RNP cleavage site. The sgRNA target site in the nestin gene is shown. Abbreviations are as follows: ITR, inverted terminal repeat; HA, homology arm; CMV, cytomegalovirus promoter; PAM, protospacer adjacent motif. (**B**) Percentage of GFP positive rat C6 cells measured by flow cytometry following delivery of different combinations of plasmid donor (800 ng), Cas9–sgRNA expression vector (800 ng), AAV donor (MOI = 100 000) and RNP (300 pmol) in the presence or absence of 1 μM Scr7. AAV donor was added to cells 16 h prior to RNP delivery. All cells were treated with 200 ng/ml of nocodazole. Values are means ($n = 3$) and error bars indicate S.D. ***$P < 0.0005$; unpaired t-tests.

tween C6 cells nucleofected with Cas9–sgRNA expression vector or RNP (Supplementary Figure S4), indicating the extent to which HDR was improved could be attributed to a potential synergy between the RNP and AAV donor vector. Sanger sequencing confirmed EGFP integration into the nestin locus (Supplementary Figure S5), further establishing the utility of AAV-RNP delivery to mediate knock-in of a reporter gene into an endogenous genomic locus via HDR.

Using AAV-RNP delivery to generate a DARPP-32-EGFP lineage reporter to monitor the generation of striatal neurons from fibroblasts

The establishment of patient-derived neurons from induced pluripotent stem cells or adult fibroblasts holds promise for disease modeling and regenerative medicine (37,46–48). However, the generation of specialized neuronal subtypes can remain challenging (49). Reporter systems that link the expression of an endogenous gene to an indicator protein allow for gene expression to be monitored in real time, thereby providing a means to optimize or develop procedures to enrich for a neural subtype. We thus asked whether AAV-RNP delivery could be leveraged to genetically tag the human dopamine- and cAMP-regulated neuronal phosphoprotein (DARPP-32) gene with a fluorescent reporter to enable the identification of neuron-like cells from human fibroblasts. DARPP-32 is part of the dopamine signaling pathway (50), as well as a marker for striatal neurons, a neuronal subtype affected in Huntington's disease.

We designed an sgRNA targeting the last exon of the DARPP-32 gene and constructed a donor template identical to the one described for the nestin gene, but with ∼1000 nucleotides of identity to the DARPP-32 locus in each homology arm and a PGK promoter to drive expression of the puromycin-resistance gene (Figure 4A). Correct targeting of the donor vector would thus produce a DARPP-32-EGFP fusion gene that would be expressed only in striatal neurons. We delivered into primary fibroblasts a high dose of DARPP-32-AAV1 donor template (MOI = 500 000) and RNP (300 pmol) complexed with a DARPP-32-targeting sgRNA. Notably, these cells were treated with aphidicolin (40), an S-phase blocker that we previously showed could enhance HDR in primary fibroblasts (19). Fibroblasts were then transduced with multiple lentiviral vectors to express miR-9/9*-124, Bcl-XL and the transcription factors CTIP2, DLX1, DLX2 and MYT1L (referred to as CDM) (Figure 4B), which together can guide the conversion of adult fibroblasts into a population of neurons functionally equivalent to striatal medium spiny neurons (MSNs) (37,51). Analysis of the DARPP-32 locus by digital droplet PCR, a method capable of quantifying the frequency of transgene insertion at a targeted locus (52,53), revealed that ∼0.5% of DARPP-32 alleles from fibroblasts treated by AAV-RNP were modified to contain EGFP before puromycin selection (Figure 4C). This corresponded to ∼5-fold increase over fibroblasts nucleofected with a plasmid donor and Cas9–sgRNA expression vector (Figure 4C). Importantly, this analysis may underestimate the frequency of HDR-mediated genome editing in the DARPP-32 gene given the difficulty of amplifying DNA fragments >1 kb in length by digital droplet PCR.

Following puromycin selection and completion of the differentiation protocol, we quantified neuronal conversion by immunostaining cells for microtubule-associated protein 2 (MAP2), a neuron-specific cytoskeletal protein, as well as DARPP-32, which is selectively expressed in MSNs. Consistent with past reports (37), we found that ∼80% of DAPI$^+$ cells were MAP2$^+$ ($n = 100$) and that ∼60% of MAP2+ cells were DARPP-32$^+$ ($n = 70$) by day 35 of the reprogramming (Figure 4D). Impressively, we found that ∼95% of DARPP-32$^+$ cells were also EGFP$^+$ ($n = 50$) (Figure 4D), indicating the ability of the EGFP reporter to accu-

Downloaded from https://academic.oup.com/nar/article-abstract/45/11/e98/3059660/Targeted-gene-knock-in-by-homology-directed-genome
by Undergraduate Library user
on 13 October 2017

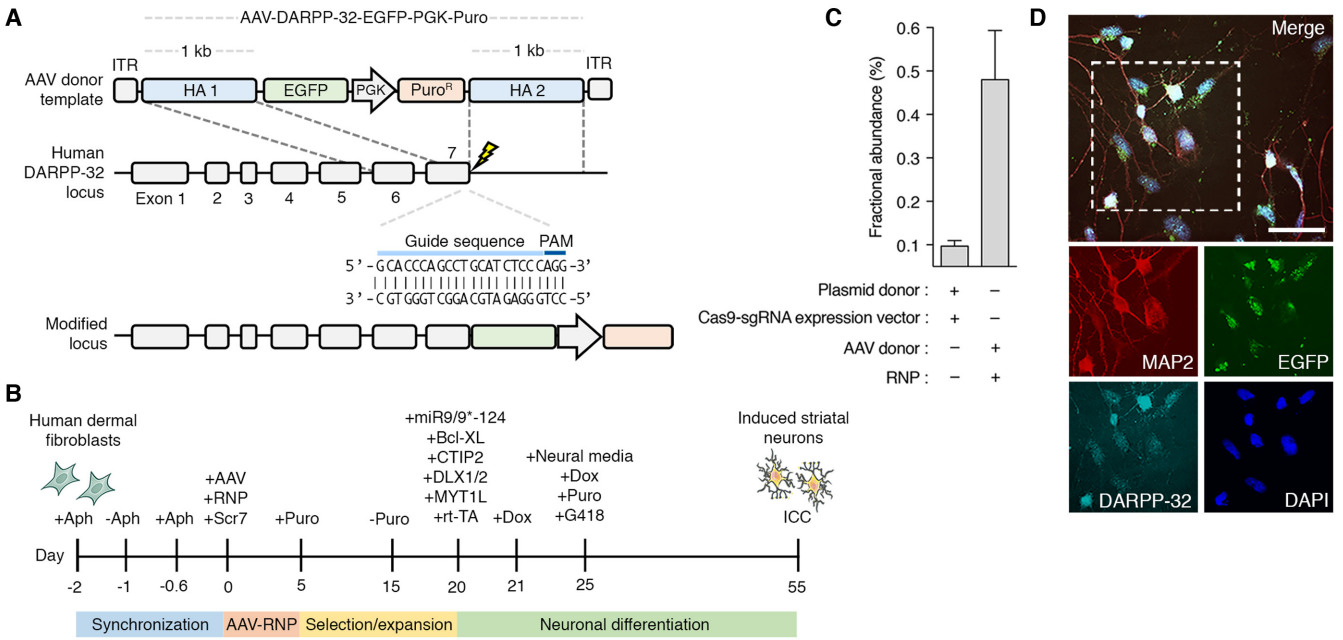

Figure 4. AAV-RNP-mediated knock-in of EGFP into the human DARPP-32 locus enables induced striatal neurons to be visualized via EGFP fluorescence. (**A**) Cartoon representation of the strategy used to tag the human DARPP-32 gene with EGFP. Lightning bolt indicates approximate position of the RNP cleavage site. The sgRNA target site in the DARPP-32 gene is shown. Abbreviations are as follows: ITR, inverted terminal repeat; HA, homology arm; CMV, cytomegalovirus promoter; PAM, protospacer adjacent motif. (**B**) Experimental workflow for generating striatal neurons from human dermal fibroblasts. AAV donor was added to cells immediately after RNP nucleofection. Abbreviations are as follows: Aph, aphidicolin; dox, doxycycline; ICC, immunocytochemistry. (**C**) Frequency of targeted integration into the DARPP-32 gene in human dermal fibroblasts following delivery of plasmid donor (800 ng) and Cas9–sgRNA expression vector (800 ng) or AAV donor (MOI = 500 000) and RNP (300 pmol), as determined by digital droplet PCR. All cells were treated with 2 μg/ml of aphidicolin and 1 μM Scr7. Values are means ($n = 3$). (**D**) ICC analysis of human dermal fibroblasts after 55 days of neural differentiation. Images were captured using identical exposure conditions. Scale bar, 50 μm.

rately track DARPP-32 expression. Importantly, no EGFP expression was observed in control puromycin-enriched fibroblasts treated with AAV-RNP, but not miR-9/9*-124, Bcl-XL and CDM (Supplementary Figure S6). Together, these results illustrate the potential of AAV-RNP to knock-in reporter genes to track neuronal differentiation.

DISCUSSION

In the present study, we demonstrate that combining RNP and AAV donor template delivery enables efficient homology-directed genome editing in mammalian cells. This method relies on two components: (i) a pre-assembled RNP complex to induce a DSB that stimulates the cellular DNA repair pathway and (ii) an AAV vector to mediate delivery of a donor template for HDR. AAV-RNP delivery thus capitalizes on the strengths of each individual platform and offers several distinct advantages over plasmid-based methods for realizing HDR-mediated genome editing, including targeted gene addition. First, compared to strategies that express both the Cas9 and its sgRNA from nucleic acids, direct delivery of a purified and pre-formed RNP complex has previously been shown to reduce the frequency of off-target effects induced by Cas9 (18–21,54), and potentially even lessens its immunogenic impact (55). This is because the RNP is quickly degraded once internalized by cells, which reduces the amount of time Cas9 has to cleave off-target sites. Second, there is no risk for insertional mutagenesis of a Cas9 expression vector with RNP delivery. And third, AAV vectors, which exhibit low pathogenicity (56,57), can promote HR at efficiencies ~10^3–10^4 higher than traditional plasmid donors or other viral vector systems (16). This natural 'recombinogenicity' has been suggested to arise from the single-stranded AAV vector genome (58) or the ITRs (59).

Despite similar levels of indel formation between cells nucleofected with RNP or the Cas9–sgRNA expression vector, we observed a >10-fold increase in HDR by AAV-RNP delivery compared to plasmid nucleofection. These results indicate a possible synergy between the RNP and AAV donor vector that may be explained by a well-timed and opportunistic interaction between the HDR repair machinery (which is activated by the RNP shortly after its internalization) and newly unpackaged single-stranded donor template. Cellular DNA repair factors, including Rad52 (which plays an important role in HR) can associate with the single-stranded AAV genome (60,61) and may also contribute to AAV-RNP-mediated HDR. Intriguingly, we observed negligible amounts of HDR when the Cas9–sgRNA expression vector was combined with the AAV donor vector. Though the exact reason for this remains unknown, it is possible that an inhibitory effect exists between the Cas9 expression vector and the AAV viral genome. Additionally, because of its ability to enhance HDR and the challenges associated with generating homology arms, AAV-RNP may prove useful for future efforts to drive HDR with donor templates

Downloaded from https://academic.oup.com/nar/article-abstract/45/11/e98/3059660/Targeted-gene-knock-in-by-homology-directed-genome
by Undergraduate Library user
on 13 October 2017

containing homology arms that are limited in size (<100 bp) (62,63).

Of note, there are reports of co-delivering an AAV donor vector with a synthetic mRNA encoding zinc-finger (64–67) and TALE nucleases (67), as well as megaTALs (68)—a hybrid nuclease consisting of an engineered homing endonuclease cleavage domain fused to a designer TALE DNA-binding domain (69). While these methods enabled gene addition, they nonetheless require engineering new protein domains for genome editing. RNPs, in contrast, can be reprogrammed by replacing the specificity-determining sequence within the sgRNA, which offers a greater ease of use compared to other genome-modifying technologies.

Consistent with our earlier studies that focused on employing RNPs in combination with recombinogenic single-stranded DNA oligonucleotides (19), we found that arresting cells at G2/M phase using the microtubule inhibitor nocodazole increased recombination efficiency. Since HR is nearly absent in the G1 phase of the cell cycle, but up-regulated during late S phase to G2 phase (70), these results underscore the importance of cell synchronization for maximizing homology-directed genome editing in mitotic cells. Fusing the Cas9 protein to post-translational regulatory domains, such as the N-terminal region of human Geminin (71,72)—a substrate for ubiquitin ligase complexes activated during the late M1 and G1 phases of the cell cycle—could further improve genome editing specificity by providing a strategy for quickly degrading Cas9 protein in non-synchronized cells.

We also illustrate the ability of AAV-RNP delivery to facilitate the creation of lineage reporters that can provide real time monitoring of cellular reprogramming. This was evidenced by our employing AAV-RNP delivery to genetically tag the endogenous DARRP-32 gene in primary human fibroblasts with the EGFP gene. Following their conversion to striatal neurons using an established approach (37,51), we visualized DARPP-32 expression via native EGFP fluorescence. Importantly, we observed a high degree of overlap between induced neurons expressing both DARPP-32 and EGFP. Although no DARPP-32 or EGFP expression was observed in control non-differentiated fibroblasts treated with AAV-RNP, we identified several cells that did not express DARPP-32 but were positive for both MAP2, which is a neuron-specific cytoskeletal protein, and EGFP. This could be due to either off-target integration of the donor construct or insufficient levels of DARPP-32 protein within correctly targeted cells for efficient detection using our anti-DARPP-32 antibody. This latter possibility indicates that lineage reporters may provide earlier detection compared to immunofluorescent staining.

Finally, AAV-RNP delivery has the potential to offer new opportunities for therapeutic genome editing (73). For example, nuclease-encoding mRNA and AAV donor templates were previously employed to facilitate correction of hereditary surfactant protein B (SP-B) deficiency in a mouse model of the disease (67). By further improving on the stability of the RNP complex and perhaps incorporating targeting modules that could promote delivery to certain tissues and cell types *in vivo*, therapeutic gene integration or correction by AAV-RNP delivery could become a reality. Similarly, RNP and AAV donor template co-delivery recently enabled *ex vivo* correction of a single-base mutation in the β-globin gene (74), which could be used to treat the β-haemoglobinopathies, including β-thalassaemia and sickle cell disease. AAV-RNP delivery could also be employed to treat neurological disorders. For example, we recently demonstrated the ability of Cas9 RNP complexes to mediate genome editing in the mouse brain following local delivery (75). This approach could be coupled with emerging methods for facilitating targeted gene addition in non-dividing cells, including homology-independent targeted integration (HITI) (76), to enable therapeutic DNA knock-in.

In conclusion, we demonstrate that combining Cas9 RNP and AAV donor delivery enables homology-directed genome editing in mammalian cells. This work thus expands on the capabilities of the RNP genome editing toolbox.

SUPPLEMENTARY DATA

Supplementary Data are available at NAR Online.

ACKNOWLEDGEMENTS

Author contribution: T.G. and B.T.S. designed the experiments. T.G., B.T.S, G.M.C.R., P.L. and F.K.E. performed the research. T.G. and B.T.S. analyzed the data. T.G., B.T.S., J.A.D. and D.V.S. wrote the manuscript.

FUNDING

Ruth L. Kirschstein National Research Service Award (NRSA) (F32GM113446) (to T.G.); F. Hoffmann-La Roche Postdoctoral Fellowship [RPF311 to B.T.S.]; Fundação para a Ciência e a Tecnologia (FCT) de Portugal [SFRH/BD/89374/2012 to G.M.C.R.]; National Institutes of Health (NIH) [R01EY022975 to D.V.S.]; Roche Pharmaceutical's Roche Alliance with Distinguished Scientists (ROADS) Fund Award (to J.A.D.); HHMI Investigator and a Paul Allen Frontiers in Science investigator (to J.A.D.). Funding for open access charge: NIH.

Conflict of interest statement. D.V.S. is an inventor on patents related to AAV vectors and co-founder of a company developing AAV vectors for clinical gene therapy. J.A.D. is employed by HHMI and works at the University at California, Berkeley. UC Berkeley and HHMI have patents pending for CRISPR technologies on which she is an inventor. J.A.D. is the executive director of the Innovative Genomics Institute at UC Berkeley and UCSF. J.A.D. is a co-founder of Editas Medicine, Intellia Therapeutics and Caribou Biosciences and a scientific advisor to Caribou, Intellia, eFFECTOR Therapeutics and Driver.

REFERENCES

1. Jinek,M., Chylinski,K., Fonfara,I., Hauer,M., Doudna,J.A. and Charpentier,E. (2012) A programmable dual-RNA-guided DNA endonuclease in adaptive bacterial immunity. *Science*, **337**, 816–821.
2. Barrangou,R. and Doudna,J.A. (2016) Applications of CRISPR technologies in research and beyond. *Nat. Biotechnol.*, **34**, 933–941.
3. Cong,L., Ran,F.A., Cox,D., Lin,S., Barretto,R., Habib,N., Hsu,P.D., Wu,X., Jiang,W., Marraffini,L.A. *et al.* (2013) Multiplex genome engineering using CRISPR/Cas systems. *Science*, **339**, 819–823.
4. Mali,P., Yang,L., Esvelt,K.M., Aach,J., Guell,M., DiCarlo,J.E., Norville,J.E. and Church,G.M. (2013) RNA-guided human genome engineering via Cas9. *Science*, **339**, 823–826.

Downloaded from https://academic.oup.com/nar/article-abstract/45/11/e98/3059660/Targeted-gene-knock-in-by-homology-directed-genome
by Undergraduate Library user
on 13 October 2017

5. Jinek,M., East,A., Cheng,A., Lin,S., Ma,E. and Doudna,J. (2013) RNA-programmed genome editing in human cells. *Elife*, **2**, e00471.
6. Carroll,D. (2014) Genome engineering with targetable nucleases. *Annu. Rev. Biochem.*, **83**, 409–439.
7. Gaj,T., Sirk,S.J., Shui,S.L. and Liu,J. (2016) Genome-editing technologies: principles and applications. *Cold Spring Harb. Perspect. Biol.*, **8**, a023754.
8. Rouet,P., Smih,F. and Jasin,M. (1994) Introduction of double-strand breaks into the genome of mouse cells by expression of a rare-cutting endonuclease. *Mol. Cell. Biol.*, **14**, 8096–8106.
9. Choulika,A., Perrin,A., Dujon,B. and Nicolas,J.F. (1995) Induction of homologous recombination in mammalian chromosomes by using the I-SceI system of Saccharomyces cerevisiae. *Mol. Cell. Biol.*, **15**, 1968–1973.
10. Bibikova,M., Golic,M., Golic,K.G. and Carroll,D. (2002) Targeted chromosomal cleavage and mutagenesis in Drosophila using zinc-finger nucleases. *Genetics*, **161**, 1169–1175.
11. Santiago,Y., Chan,E., Liu,P.Q., Orlando,S., Zhang,L., Urnov,F.D., Holmes,M.C., Guschin,D., Waite,A., Miller,J.C. *et al.* (2008) Targeted gene knockout in mammalian cells by using engineered zinc-finger nucleases. *Proc. Natl. Acad. Sci. U.S.A.*, **105**, 5809–5814.
12. Porteus,M.H. and Baltimore,D. (2003) Chimeric nucleases stimulate gene targeting in human cells. *Science*, **300**, 763.
13. Urnov,F.D., Miller,J.C., Lee,Y.L., Beausejour,C.M., Rock,J.M., Augustus,S., Jamieson,A.C., Porteus,M.H., Gregory,P.D. and Holmes,M.C. (2005) Highly efficient endogenous human gene correction using designed zinc-finger nucleases. *Nature*, **435**, 646–651.
14. Moehle,E.A., Rock,J.M., Lee,Y.L., Jouvenot,Y., DeKelver,R.C., Gregory,P.D., Urnov,F.D. and Holmes,M.C. (2007) Targeted gene addition into a specified location in the human genome using designed zinc finger nucleases. *Proc. Natl. Acad. Sci. U.S.A.*, **104**, 3055–3060.
15. Stewart,M.P., Sharei,A., Ding,X., Sahay,G., Langer,R. and Jensen,K.F. (2016) In vitro and ex vivo strategies for intracellular delivery. *Nature*, **538**, 183–192.
16. Russell,D.W. and Hirata,R.K. (1998) Human gene targeting by viral vectors. *Nat. Genet.*, **18**, 325–330.
17. Heyer,W.D., Ehmsen,K.T. and Liu,J. (2010) Regulation of homologous recombination in eukaryotes. *Annu. Rev. Genet.*, **44**, 113–139.
18. Kim,S., Kim,D., Cho,S.W., Kim,J. and Kim,J.S. (2014) Highly efficient RNA-guided genome editing in human cells via delivery of purified Cas9 ribonucleoproteins. *Genome Res.*, **24**, 1012–1019.
19. Lin,S., Staahl,B.T., Alla,R.K. and Doudna,J.A. (2014) Enhanced homology-directed human genome engineering by controlled timing of CRISPR/Cas9 delivery. *Elife*, **3**, e04766.
20. Liu,J., Gaj,T., Yang,Y., Wang,N., Shui,S., Kim,S., Kanchiswamy,C.N., Kim,J.S. and Barbas,C.F. 3rd (2015) Efficient delivery of nuclease proteins for genome editing in human stem cells and primary cells. *Nat. Protoc.*, **10**, 1842–1859.
21. Zuris,J.A., Thompson,D.B., Shu,Y., Guilinger,J.P., Bessen,J.L., Hu,J.H., Maeder,M.L., Joung,J.K., Chen,Z.Y. and Liu,D.R. (2015) Cationic lipid-mediated delivery of proteins enables efficient protein-based genome editing in vitro and in vivo. *Nat. Biotechnol.*, **33**, 73–80.
22. Wang,M., Zuris,J.A., Meng,F., Rees,H., Sun,S., Deng,P., Han,Y., Gao,X., Pouli,D., Wu,Q. *et al.* (2016) Efficient delivery of genome-editing proteins using bioreducible lipid nanoparticles. *Proc. Natl. Acad. Sci. U.S.A.*, **113**, 2868–2873.
23. Gaj,T., Guo,J., Kato,Y., Sirk,S.J. and Barbas,C.F. 3rd (2012) Targeted gene knockout by direct delivery of zinc-finger nuclease proteins. *Nat. Methods*, **9**, 805–807.
24. Liu,J., Gaj,T., Wallen,M.C. and Barbas,C.F. 3rd (2015) Improved cell-penetrating zinc-finger nuclease proteins for precision genome engineering. *Mol. Ther. Nucleic Acids*, **4**, e232.
25. Gaj,T., Liu,J., Anderson,K.E., Sirk,S.J. and Barbas,C.F. 3rd (2014) Protein delivery using Cys2-His2 zinc-finger domains. *ACS Chem. Biol.*, **9**, 1662–1667.
26. Liu,J., Gaj,T., Patterson,J.T., Sirk,S.J. and Barbas,C.F. 3rd (2014) Cell-penetrating peptide-mediated delivery of TALEN proteins via bioconjugation for genome engineering. *PLoS One*, **9**, e85755.
27. Chen,F., Pruett-Miller,S.M., Huang,Y., Gjoka,M., Duda,K., Taunton,J., Collingwood,T.N., Frodin,M. and Davis,G.D. (2011) High-frequency genome editing using ssDNA oligonucleotides with zinc-finger nucleases. *Nat. Methods*, **8**, 753–755.
28. Hendel,A., Bak,R.O., Clark,J.T., Kennedy,A.B., Ryan,D.E., Roy,S., Steinfeld,I., Lunstad,B.D., Kaiser,R.J., Wilkens,A.B. *et al.* (2015) Chemically modified guide RNAs enhance CRISPR-Cas genome editing in human primary cells. *Nat. Biotechnol.*, **33**, 985–989.
29. Kotterman,M.A., Chalberg,T.W. and Schaffer,D.V. (2015) Viral vectors for gene therapy: translational and clinical outlook. *Annu. Rev. Biomed. Eng.*, **17**, 63–89.
30. Hirata,R., Chamberlain,J., Dong,R. and Russell,D.W. (2002) Targeted transgene insertion into human chromosomes by adeno-associated virus vectors. *Nat. Biotechnol.*, **20**, 735–738.
31. Khan,I.F., Hirata,R.K. and Russell,D.W. (2011) AAV-mediated gene targeting methods for human cells. *Nat. Protoc.*, **6**, 482–501.
32. Gaj,T., Epstein,B.E. and Schaffer,D.V. (2016) Genome engineering using adeno-associated virus: basic and clinical research applications. *Mol. Ther.*, **24**, 458–464.
33. Asuri,P., Bartel,M.A., Vazin,T., Jang,J.H., Wong,T.B. and Schaffer,D.V. (2012) Directed evolution of adeno-associated virus for enhanced gene delivery and gene targeting in human pluripotent stem cells. *Mol. Ther.*, **20**, 329–338.
34. Hockemeyer,D., Soldner,F., Beard,C., Gao,Q., Mitalipova,M., DeKelver,R.C., Katibah,G.E., Amora,R., Boydston,E.A., Zeitler,B. *et al.* (2009) Efficient targeting of expressed and silent genes in human ESCs and iPSCs using zinc-finger nucleases. *Nat. Biotechnol.*, **27**, 851–857.
35. Gaj,T. and Schaffer,D.V. (2016) Adeno-associated virus-mediated delivery of CRISPR-Cas systems for genome engineering in mammalian cells. *Cold Spring Harb. Protoc.*, doi:10.1101/pdb.prot086868.
36. Guschin,D.Y., Waite,A.J., Katibah,G.E., Miller,J.C., Holmes,M.C. and Rebar,E.J. (2010) A rapid and general assay for monitoring endogenous gene modification. *Methods Mol. Biol.*, **649**, 247–256.
37. Victor,M.B., Richner,M., Hermanstyne,T.O., Ransdell,J.L., Sobieski,C., Deng,P.Y., Klyachko,V.A., Nerbonne,J.M. and Yoo,A.S. (2014) Generation of human striatal neurons by microRNA-dependent direct conversion of fibroblasts. *Neuron*, **84**, 311–323.
38. Zou,J., Maeder,M.L., Mali,P., Pruett-Miller,S.M., Thibodeau-Beganny,S., Chou,B.K., Chen,G., Ye,Z., Park,I.H., Daley,G.Q. *et al.* (2009) Gene targeting of a disease-related gene in human induced pluripotent stem and embryonic stem cells. *Cell Stem Cell*, **5**, 97–110.
39. Ellis,B.L., Hirsch,M.L., Barker,J.C., Connelly,J.P., Steininger,R.J. 3rd and Porteus,M.H. (2013) A survey of ex vivo/in vitro transduction efficiency of mammalian primary cells and cell lines with Nine natural adeno-associated virus (AAV1-9) and one engineered adeno-associated virus serotype. *Virol. J.*, **10**, 74.
40. Jackman,J. and O'Connor,P.M. (2001) Methods for synchronizing cells at specific stages of the cell cycle. *Curr. Protoc. Cell Biol.*, doi:10.1002/0471143030.cb0803s00.
41. Srivastava,M., Nambiar,M., Sharma,S., Karki,S.S., Goldsmith,G., Hegde,M., Kumar,S., Pandey,M., Singh,R.K., Ray,P. *et al.* (2012) An inhibitor of nonhomologous end-joining abrogates double-strand break repair and impedes cancer progression. *Cell*, **151**, 1474–1487.
42. Chu,V.T., Weber,T., Wefers,B., Wurst,W., Sander,S., Rajewsky,K. and Kuhn,R. (2015) Increasing the efficiency of homology-directed repair for CRISPR-Cas9-induced precise gene editing in mammalian cells. *Nat. Biotechnol.*, **33**, 543–548.
43. Maruyama,T., Dougan,S.K., Truttmann,M.C., Bilate,A.M., Ingram,J.R. and Ploegh,H.L. (2015) Increasing the efficiency of precise genome editing with CRISPR-Cas9 by inhibition of nonhomologous end joining. *Nat. Biotechnol.*, **33**, 538–542.
44. Ashton,R.S., Conway,A., Pangarkar,C., Bergen,J., Lim,K.I., Shah,P., Bissell,M. and Schaffer,D.V. (2012) Astrocytes regulate adult hippocampal neurogenesis through ephrin-B signaling. *Nat. Neurosci.*, **15**, 1399–1406.
45. Chang,K.W., Huang,Y.L., Wong,Z.R., Su,P.H., Huang,B.M., Ju,T.K. and Yang,H.Y. (2013) Fibroblast growth factor-2 up-regulates the expression of nestin through the Ras-Raf-ERK-Sp1 signaling axis in C6 glioma cells. *Biochem. Biophys. Res. Commun.*, **434**, 854–860.
46. Takahashi,K. and Yamanaka,S. (2006) Induction of pluripotent stem cells from mouse embryonic and adult fibroblast cultures by defined factors. *Cell*, **126**, 663–676.

Downloaded from https://academic.oup.com/nar/article-abstract/45/11/e98/3059660/Targeted-gene-knock-in-by-homology-directed-genome
by Undergraduate Library user
on 13 October 2017

47. Takahashi,K., Tanabe,K., Ohnuki,M., Narita,M., Ichisaka,T., Tomoda,K. and Yamanaka,S. (2007) Induction of pluripotent stem cells from adult human fibroblasts by defined factors. *Cell*, **131**, 861–872.
48. Yu,J., Vodyanik,M.A., Smuga-Otto,K., Antosiewicz-Bourget,J., Frane,J.L., Tian,S., Nie,J., Jonsdottir,G.A., Ruotti,V., Stewart,R. *et al.* (2007) Induced pluripotent stem cell lines derived from human somatic cells. *Science*, **318**, 1917–1920.
49. Hu,B.Y., Weick,J.P., Yu,J., Ma,L.X., Zhang,X.Q., Thomson,J.A. and Zhang,S.C. (2010) Neural differentiation of human induced pluripotent stem cells follows developmental principles but with variable potency. *Proc. Natl. Acad. Sci. U.S.A.*, **107**, 4335–4340.
50. Svenningsson,P., Nishi,A., Fisone,G., Girault,J.A., Nairn,A.C. and Greengard,P. (2004) DARPP-32: an integrator of neurotransmission. *Annu. Rev. Pharmacol. Toxicol.*, **44**, 269–296.
51. Richner,M., Victor,M.B., Liu,Y., Abernathy,D. and Yoo,A.S. (2015) MicroRNA-based conversion of human fibroblasts into striatal medium spiny neurons. *Nat. Protoc.*, **10**, 1543–1555.
52. Miyaoka,Y., Chan,A.H., Judge,L.M., Yoo,J., Huang,M., Nguyen,T.D., Lizarraga,P.P., So,P.L. and Conklin,B.R. (2014) Isolation of single-base genome-edited human iPS cells without antibiotic selection. *Nat. Methods*, **11**, 291–293.
53. Mock,U., Hauber,I. and Fehse,B. (2016) Digital PCR to assess gene-editing frequencies (GEF-dPCR) mediated by designer nucleases. *Nat. Protoc.*, **11**, 598–615.
54. Ramakrishna,S., Kwaku Dad,A.B., Beloor,J., Gopalappa,R., Lee,S.K. and Kim,H. (2014) Gene disruption by cell-penetrating peptide-mediated delivery of Cas9 protein and guide RNA. *Genome Res.*, **24**, 1020–1027.
55. Chew,W.L., Tabebordbar,M., Cheng,J.K., Mali,P., Wu,E.Y., Ng,A.H., Zhu,K., Wagers,A.J. and Church,G.M. (2016) A multifunctional AAV-CRISPR-Cas9 and its host response. *Nat. Methods*, **13**, 868–874.
56. Nathwani,A.C., Reiss,U.M., Tuddenham,E.G., Rosales,C., Chowdary,P., McIntosh,J., Della Peruta,M., Lheriteau,E., Patel,N., Raj,D. *et al.* (2014) Long-term safety and efficacy of factor IX gene therapy in hemophilia B. *N. Engl. J. Med.*, **371**, 1994–2004.
57. Gaudet,D., Methot,J., Dery,S., Brisson,D., Essiembre,C., Tremblay,G., Tremblay,K., de Wal,J., Twisk,J., van den Bulk,N. *et al.* (2013) Efficacy and long-term safety of alipogene tiparvovec (AAV1-LPLS447X) gene therapy for lipoprotein lipase deficiency: an open-label trial. *Gene Ther.*, **20**, 361–369.
58. Hirata,R.K. and Russell,D.W. (2000) Design and packaging of adeno-associated virus gene targeting vectors. *J. Virol.*, **74**, 4612–4620.
59. Hirsch,M.L. (2015) Adeno-associated virus inverted terminal repeats stimulate gene editing. *Gene Ther.*, **22**, 190–195.
60. Zentilin,L., Marcello,A. and Giacca,M. (2001) Involvement of cellular double-stranded DNA break binding proteins in processing of the recombinant adeno-associated virus genome. *J. Virol.*, **75**, 12279–12287.
61. Choi,V.W., McCarty,D.M. and Samulski,R.J. (2006) Host cell DNA repair pathways in adeno-associated viral genome processing. *J. Virol.*, **80**, 10346–10356.
62. Orlando,S.J., Santiago,Y., DeKelver,R.C., Freyvert,Y., Boydston,E.A., Moehle,E.A., Choi,V.M., Gopalan,S.M., Lou,J.F., Li,J. *et al.* (2010) Zinc-finger nuclease-driven targeted integration into mammalian genomes using donors with limited chromosomal homology. *Nucleic Acids Res.*, **38**, e152.
63. Arbab,M., Srinivasan,S., Hashimoto,T., Geijsen,N. and Sherwood,R.I. (2015) Cloning-free CRISPR. *Stem Cell Rep.*, **5**, 908–917.
64. Wang,J., Exline,C.M., DeClercq,J.J., Llewellyn,G.N., Hayward,S.B., Li,P.W., Shivak,D.A., Surosky,R.T., Gregory,P.D., Holmes,M.C. *et al.* (2015) Homology-driven genome editing in hematopoietic stem and progenitor cells using ZFN mRNA and AAV6 donors. *Nat. Biotechnol.*, **33**, 1256–1263.
65. Wang,J., DeClercq,J.J., Hayward,S.B., Li,P.W., Shivak,D.A., Gregory,P.D., Lee,G. and Holmes,M.C. (2016) Highly efficient homology-driven genome editing in human T cells by combining zinc-finger nuclease mRNA and AAV6 donor delivery. *Nucleic Acids Res.*, **44**, e30.
66. De Ravin,S.S., Reik,A., Liu,P.Q., Li,L., Wu,X., Su,L., Raley,C., Theobald,N., Choi,U., Song,A.H. *et al.* (2016) Targeted gene addition in human CD34(+) hematopoietic cells for correction of X-linked chronic granulomatous disease. *Nat. Biotechnol.*, **34**, 424–429.
67. Mahiny,A.J., Dewerth,A., Mays,L.E., Alkhaled,M., Mothes,B., Malaeksefat,E., Loretz,B., Rottenberger,J., Brosch,D.M., Reautschnig,P. *et al.* (2015) In vivo genome editing using nuclease-encoding mRNA corrects SP-B deficiency. *Nat. Biotechnol.*, **33**, 584–586.
68. Sather,B.D., Romano Ibarra,G.S., Sommer,K., Curinga,G., Hale,M., Khan,I.F., Singh,S., Song,Y., Gwiazda,K., Sahni,J. *et al.* (2015) Efficient modification of CCR5 in primary human hematopoietic cells using a megaTAL nuclease and AAV donor template. *Sci. Transl. Med.*, **7**, 307ra156.
69. Boissel,S., Jarjour,J., Astrakhan,A., Adey,A., Gouble,A., Duchateau,P., Shendure,J., Stoddard,B.L., Certo,M.T., Baker,D. *et al.* (2014) megaTALs: a rare-cleaving nuclease architecture for therapeutic genome engineering. *Nucleic Acids Res.*, **42**, 2591–2601.
70. Branzei,D. and Foiani,M. (2008) Regulation of DNA repair throughout the cell cycle. *Nat. Rev. Mol. Cell Biol.*, **9**, 297–308.
71. Gutschner,T., Haemmerle,M., Genovese,G., Draetta,G.F. and Chin,L. (2016) Post-translational regulation of Cas9 during G1 enhances homology-directed repair. *Cell Rep.*, **14**, 1555–1566.
72. Howden,S.E., McColl,B., Glaser,A., Vadolas,J., Petrou,S., Little,M.H., Elefanty,A.G. and Stanley,E.G. (2016) A Cas9 variant for efficient generation of indel-free knockin or gene-corrected human pluripotent stem cells. *Stem Cell Rep.*, **7**, 508–517.
73. Maeder,M.L. and Gersbach,C.A. (2016) Genome-editing technologies for gene and cell therapy. *Mol. Ther.*, **24**, 430–446.
74. Dever,D.P., Bak,R.O., Reinisch,A., Camarena,J., Washington,G., Nicolas,C.E., Pavel-Dinu,M., Saxena,N., Wilkens,A.B., Mantri,S. *et al.* (2016) CRISPR/Cas9 beta-globin gene targeting in human haematopoietic stem cells. *Nature*, **539**, 384–389.
75. Staahl,B.T., Benekareddy,M., Coulon-Bainier,C., Banfal,A.A., Floor,S.N., Sabo,J.K., Urnes,C., Munares,G.A., Ghosh,A. and Doudna,J.A. (2017) Efficient genome editing in the mouse brain by local delivery of engineered Cas9 ribonucleoprotein complexes. *Nat. Biotechnol.*, doi:10.1038/nbt.3806.
76. Suzuki,K., Tsunekawa,Y., Hernandez-Benitez,R., Wu,J., Zhu,J., Kim,E.J., Hatanaka,F., Yamamoto,M., Araoka,T., Li,Z. *et al.* (2016) In vivo genome editing via CRISPR/Cas9 mediated homology-independent targeted integration. *Nature*, **540**, 144–149.

Downloaded from https://academic.oup.com/nar/article-abstract/45/11/e98/3059660/Targeted-gene-knock-in-by-homology-directed-genome
by Undergraduate Library user
on 13 October 2017